

1 Impacts of Pavement Condition on Fine Sediment Particle Load in Roadway Stormwater Runoff

2

3

4

5

6

7

8 Hyun-Min Hwang^{1*}, Russell Wigart², Andrea Buxton³

9

10 ¹Department of Environmental Science, Texas Southern University, Houston, Texas, USA,

11 77094

12 ²Tahoe Planning and Stormwater Division, El Dorado County, California, USA

13 ³Tahoe Resource Conservation District, South Lake Tahoe, California, USA

14

15

16 *Corresponding author: hyun-min.hwang@tsu.edu

17 **ABSTRACT:** Pavement deterioration has not been recognized as a major source of fine
18 sediment particles (FSP) that should be mitigated to help improve the clarity of Lake Tahoe. This
19 study investigated impacts of asphalt pavement condition on FSP loads in roadway stormwater
20 runoff in South Lake Tahoe. Stormwater samples were collected before and after pavement
21 rehabilitation. Pavement condition index was improved from 29 (poor) to 99 (excellent) after the
22 rehabilitation. Samples were analyzed for elements and organic markers (e.g., hopanes) to
23 determine the contributions of FSP from major sources using a chemical mass balance model.
24 Volume weighted mean concentrations and annual loads of FSP declined from 53.1 mg/L to 8.57
25 mg/L and from 293 kg to 36.7 kg, respectively, equivalent to 756 Lake Clarity Credits per 1 km²
26 of pavement. Before pavement rehabilitation, pavement wear was the primary source of FSP in
27 stormwater runoff. Volume weighted mean concentration of FSP from pavement wear, native
28 surface soil, and traction abrasives declined from 22.4 mg/L to 2.12 mg/L, from 17.5 mg/L to
29 3.65 mg/L, and from 9.23 mg/L to 0.76 mg/L, respectively, indicating that pavement condition
30 improvement should be considered for water quality management to restore the extraordinary
31 clarity of Lake Tahoe.

32

33 **KEY WORDS:** Fine sediment particles, Source apportionment, Stormwater runoff, Pavement
34 condition, Lake clarity credit

35

36 **SYNOPSIS**

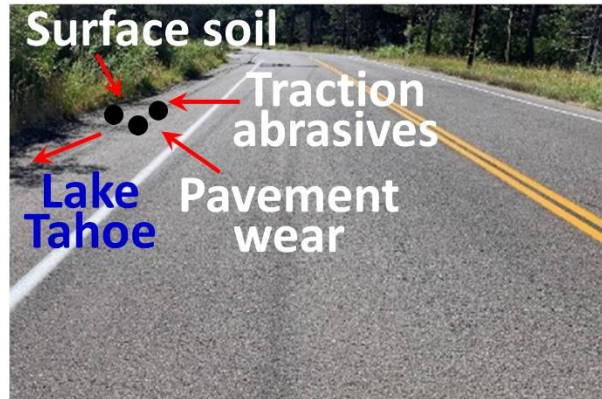
37 Pavement condition improvement significantly reduced fine sediment particles in stormwater
38 runoff and should be considered for water quality management in order to restore Lake Tahoe
39 clarity.

- **Fine Sediment Particle**



Before pavement rehabilitation

← Stormwater Runoff



After pavement rehabilitation

43 INTRODUCTION

44 Lake Tahoe, an alpine lake in the Sierra Nevada of the U.S., was designated as an
45 Outstanding National Resource Water under the federal Clean Water Act's Antidegradation
46 Policy because of its world-famous crystal-clear water. However, lake clarity has declined
47 significantly over the last several decades (Figure S1). Secchi depth, a measure of water clarity,
48 was nearly 30 meters when it was first measured in 1968 but has decreased to approximately 18
49 meters in 2020. One of the main reasons is an increase of fine sediment particles (FSP) smaller
50 than 16 μm that account for 67% of the light scattered or absorbed in the Lake Tahoe water
51 column.^{1,2} To restore Lake Tahoe's historic water transparency to 30 meters by 2076, the Lake
52 Tahoe Total Maximum Daily Load (TMDL) was adopted in 2010.³

53 Stormwater runoff from urban uplands was estimated to account for approximately 70% of
54 the total FSP entering Lake Tahoe³, suggesting that a reduction in FSP input from roadway
55 runoff is a critical mitigation strategy for improving Lake Tahoe's famed clarity. In the last two
56 decades, traction abrasives have received special attention as a dominant source of FSP in
57 roadway stormwater runoff, and many efforts have been made by municipal jurisdictions in the
58 Lake Tahoe Basin.^{4, 5} For example, El Dorado County has reduced annual traction abrasive
59 application by 60% since the early 2000s (Figure S2).⁶ Additionally, traction abrasives (e.g.,
60 Washoe sand) are washed by the vendor prior to sale to remove FSP.⁶ Despite these efforts,
61 significant reductions in FSP loads in stormwater runoff and significant improvement of Lake
62 Tahoe clarity have not been fully observed over the last 20 years (Figure S1), indicating that
63 sources other than traction abrasives contribute a large fraction of the FSP in roadway
64 stormwater runoff.

65 Previous studies found that asphalt pavement wear accounted for 20-25% of FSP in
66 stormwater runoff collected from a site in the Lake Tahoe Basin.⁷ Heavy machinery such as
67 snow plows and rotary snow blowers equipped with steel cutting edges are expected to produce
68 large amounts of FSP because they damage the asphalt pavement surface during removal of
69 snow and ice from roads (Figures S3 and S4). However, the impacts of pavement surface
70 condition on FSP loads in stormwater runoff have not been fully investigated in the Lake Tahoe
71 Basin. As a result, both States of California and Nevada and local agencies have not considered
72 generation of FSP from pavement deterioration and its impact on water quality as a factor in
73 evaluating cost-effectiveness of road asset maintenance strategies or crediting associated with the
74 Tahoe TMDL.

75 This study collected stormwater runoff samples from Elks Club Drive in South Lake Tahoe,
76 California before and after the placement of new asphalt overlay to investigate the impacts of
77 pavement condition improvement on FSP loads from major sources, including pavement wear,
78 traction abrasives, natural soil from sidehills, and vegetation debris. A significant reduction in
79 FSP in stormwater runoff was anticipated after the pavement rehabilitation through less
80 contribution from pavement materials and less accumulation of traction abrasives in cracks from
81 deteriorating pavement.

82

83 **MATERIALS AND METHODS**

84 **Study Site.** The County of El Dorado, California, USA installed new asphalt overlay (1.3 km)
85 on Elks Club Drive in the summer of 2018 to improve road sweeping efficiency and reduce air
86 pollution and stormwater pollution. This road surface rehabilitation provided an ideal
87 opportunity to investigate the effects of pavement condition improvement on FSP load reduction

88 in stormwater runoff. Reducing FSP loads is one of the objectives of the Lake Tahoe
89 Environmental Improvement Program to restore the environmental health of Lake Tahoe.⁸ Elks
90 Club Drive is identified as a major collector road that traverses a residential neighborhood
91 connecting Pioneer Trail to State Highway 50 in south of the City of South Lake Tahoe (Figure
92 S5). Prior to completion of the overlay, pavement condition index (PCI) of Elks Club Drive was
93 determined based on visual surveys of the types and severity of distresses on the pavement
94 surface. PCI is a numerical value, ranging from 0 to 100, that represents the worst and best
95 possible pavement conditions, respectively.⁹ The pavement condition of Elks Club Drive was
96 poor (Figure S6) with the PCI of 29 before placement of the new asphalt overlay. Significant
97 portions of the pavement were covered in cracks and potholes. After the placement of the asphalt
98 overlay, the pavement condition was changed to excellent with the PCI of 99 (Figure S6).

99 Total lengths of Elks Club Drive that contributed runoff to the sampling stations were 580 m
100 and 520 m in years 1 (2017-2018) and 2 (2018-2019), respectively. The total width of Elks Club
101 Drive was 10.4 m and 11.3 m in years 1 and 2, respectively. The tributary width includes pavement,
102 shoulders on both sides of the pavement, and a ditch on the north side of the road. A pavement
103 surface slope survey indicated that 70% of stormwater runoff ran toward the northern side where
104 the sampling station was installed. Five side streets that feed into Elks Club Drive also contributed
105 runoff to the sampling stations. The total length and width of the side streets that contributed runoff
106 were 1.27 km and 9.1 m, respectively. Road rehabilitation was not performed on the side streets,
107 and thus, surface area and pavement condition of the side streets were virtually equivalent in both
108 years.

109

110 **Sample Collection.** Stormwater runoff samples were collected before (year 1: between October
111 2017 and May 2018) and after (year 2: between October 2018 and May 2019) pavement
112 rehabilitation. Stormwater runoff samples were collected during 7 and 12 events in years 1 and 2,
113 respectively (Table 1). Only runoff produced by precipitation was collected. Runoff produced by
114 snowmelt was not collected because it was too clean for particle analysis. Snowmelt runoff is
115 defined as runoff produced by melting snow accumulated on adjacent sidehills and/or emerging
116 groundwater.

117 Automated sampling stations were installed in the drainage ditch on the north side of Elks
118 Club Drive (Figure S7). The locations of the sampling stations in year 1 and year 2 were slightly
119 different. In year 2, the sampling station was moved 60 m east of the point used in year 1. A
120 Tracom (Atlanta, GA, USA) Palmer Bowlus fiberglass flume instrumented with a pressure
121 transducer to measure water level, an FTS (Victoria, BC, Canada) DTS-12 digital turbidity
122 sensor, and a Teledyne (Lincoln, NE, USA) ISCO 6712 automated sampler were installed in the
123 drainage ditch. Stormwater runoff samples were collected using the ISCO sampler in twenty-four
124 1 L bottles. The ISCO sampler was programmed to fill one bottle every 8,500 L or 14,200 L across
125 the entire hydrograph for each runoff event sampled depending on the size of the storm. Sample
126 collection duration, which is time between the first sample and the last sample, of each event
127 ranged from 6 hours to 135 hours. Water level and turbidity of the runoff were measured on site
128 every 5 minutes from October 1 to September 30 in both years. Water levels were converted to
129 flow rates using an equation provided by flume manufacturer.

130 Source samples, including native surface soils and vegetation debris from hillside, traction
131 abrasive, and pavement cores were collected for chemical analysis. Atmospheric dry deposition
132 was not collected for this study. Trace element concentrations measured in atmospheric dry

133 deposition samples collected previously at a site close to Elks Club Drive were adopted for this
 134 study.⁷ The previous study reported that local atmospheric dry deposition accounted for less than
 135 3% of FSP load in roadway stormwater runoff.⁷

136

137 **Table 1.** FSP concentrations (mg/L) in roadway stormwater runoff collected from Elks Club Drive
 138 before (year 1) and after (year 2) pavement condition improvement.

139

Year 1		Year 2	
Collection date	Concentration	Collection date	Concentration
11/15/2017	27.8	11/23/2018	3.21
1/6/2018	70.9	11/27/2018	8.52
3/13/2018	19.1	1/16/2019	5.45
3/20/2018	79.2	1/20/2019	9.42
4/6/2018	60.5	2/2/2019	12.1
5/24/2018	297*	2/13/2019	8.94
5/25/2018	26.9	3/5/2019	3.06
		3/27/2019	21.0*
		4/2/2019	9.35
		4/8/2019	6.40
		5/16/2019	1.70
		5/26/2019	1.54
Arithmetic mean	47.4	Arithmetic mean	6.34
Standard deviation	25.9	Standard deviation	3.60
Volume weighted mean	53.1	Volume weighted mean	8.57

140

141 *Outliers. Arithmetic mean concentrations were calculated without outliers.

142

143

144 **Separation of Fine Sediment Particles.** Stormwater runoff samples collected in plastic
145 bottles were transported to the laboratory and passed through a stainless sieve (20 μm) to remove
146 particles greater than 20 μm . Sieved water was combined in glass bottles (4 L) and kept
147 unagitated at room temperature for at least 24 hours to ensure FSP settled to the bottom. A
148 previous study showed that more than 99% of fine sediment particles settled to bottom when
149 kept unagitated for 24 hours.⁷ Supernatant was removed using a siphon. The bottom layer,
150 enriched with FSP, was filtered through Whatman (Maidstone, UK) acid treated TCLP filter
151 papers. The filter papers with FSP were dried in an oven (60 $^{\circ}\text{C}$) for 24 hours and the weight of
152 the filter papers were measured using a balance that can measure to 0.0001 g. A portion of the
153 asphalt core top layer was dissolved in dichloromethane to separate binder and aggregates.
154 Traction abrasive, pavement aggregate, and vegetation debris were gently ground and sieved
155 using a stainless sieve (20 μm) to collect particles smaller than 20 μm . Surface soil from hillside
156 was sieved using a stainless sieve (20 μm) without grinding. The filter papers and the sieved
157 source samples were stored in a freezer (-20 $^{\circ}\text{C}$) until chemical analysis was performed.

158

159 **Chemical Analysis.** Each glass fiber filter with FSP was split into two or four fractions to be
160 analyzed for trace elements, including aluminum (Al), arsenic (As), cadmium (Cd), chromium
161 (Cr) copper (Cu), iron (Fe), lead (Pb), nickel (Ni), vanadium (V), and zinc (Zn), in the FSP. A
162 fraction of the filter was placed in a polypropylene bottle (15 mL) and digested using
163 concentrated nitric acid for 24 hours and digested again using hydrogen peroxide for 24 hours to
164 extract trace elements from FSP. Sieved source samples (0.05 g) were also digested using the
165 same procedure. Digested samples were then centrifuged, and an aliquot of supernatant was
166 diluted 5 times using deionized water made by a Milli-Q ultrapure water system before

167 instrumental analysis. Trace elements in the diluted water were analyzed and quantified using
168 Agilent (Santa Clara, CA, USA) 7900 inductively coupled plasma-mass spectrometer.

169 One or more fractions of each glass fiber filter were placed in a Teflon tube (40 mL) and
170 extracted with 35 mL of dichloromethane on a rotating tumbler for 24 hours and centrifuged at
171 2,000 rpm for 10 minutes to extract organic markers from the FSP. The top solvent layer was
172 slowly transferred into a glass concentration tube. Extraction with dichloromethane was repeated
173 twice more and solvent extracts were combined and concentrated down to 5 mL of hexane.
174 Asphalt binder in small pieces of pavement was also extracted using dichloromethane and
175 concentrated down to 5 mL of hexane. The other source samples were not extracted using
176 dichloromethane because they don't contain target organic markers. The concentrated extract
177 was filtered through a glass wool packed filter. The final volume of extract was adjusted to 5
178 mL, and an internal standard (d_{10} -pyrene) was added. Organic markers, including alkanes,
179 hopanes, and steranes, were analyzed using Agilent (Santa Clara, CA, USA) 5977B gas
180 chromatograph-mass spectrometer.

181 Each sample batch included a procedural blank, a filter paper blank and a sample duplicate.
182 National Institute of Standards and Technology standard reference material (NIST SRM) 2709a
183 (San Joaquin soil for trace element concentrations) was also included in each batch to validate
184 the accuracy of trace element quantification. Recovery rates of trace elements were between 75%
185 and 96% for all measured elements except Al, Cr, Pb, and V. Recovery rates observed in this
186 study were very similar to those reported by NIST.¹⁰

187

188 **Chemical Mass Balance Model.** The contribution of FSP from each source was estimated
189 using the chemical mass balance (CMB) model (Eq. 1),

$$C_i = \sum_{j=1}^p a_{ij} S_j, i=1, n \quad (\text{Eq. 1})$$

190
191 where C_i is a concentration (mg/L) of a chemical i in stormwater runoff, a_{ij} is a concentration
192 (mg/L) of chemical i in source j , S_j is a mass concentration (e.g., %) contributed by source j , p is
193 number of sources, and n is number of chemicals with $n \geq p$. Concentrations of the organic
194 markers were used to estimate the contribution from asphalt binder and concentrations of the
195 trace elements were used to estimate the contribution from other sources. Although the
196 contribution from tire, brake pad, tire weight balance wear particles was much less than 1%,
197 these also included in the CMB model because these sources are highly enriched with Zn, Cu,
198 and Pb.

199

200 **RESULTS AND DISCUSSION**

201 **Runoff volume.** Annual cumulative runoff volumes, including both stormwater and snowmelt,
202 that passed through the sampling station were 11,410 m³ in year 1 and 10,300 m³ in year 2.
203 Considering almost the same precipitation depth in both years (61 cm in year 1 and 62 cm in year
204 2) and a slightly shorter contributing pavement length in year 2 (580 m in year 1 and 520 m in
205 year 2), pavement rehabilitation did not substantially influence total runoff volume. However,
206 when the total runoff volumes were split into stormwater and snowmelt, significant differences
207 were observed between years 1 and 2. Annual cumulative volumes of stormwater runoff were
208 5,720 m³ and 3,150 m³ in years 1 and 2, respectively, and annual cumulative snowmelt runoff
209 volumes were 5,690 m³ and 7,150 m³ in years 1 and 2, respectively. This difference is likely
210 attributable to different precipitation patterns between years 1 and 2. Ranges and patterns of

211 ambient atmospheric temperature in year 1 and 2 were very similar. However, precipitation
212 patterns were different. In year 1, about 30% (by volume) of the precipitation occurred between
213 December 1 and March 31, when ambient temperatures are frequently cold enough to produce
214 little to no runoff. In year 2, about 70% (by volume) of precipitation occurred between December
215 1 and March 31 (Figure S8). This difference in precipitation timing likely explains the 45 %
216 lower stormwater runoff volume and the 25% greater snowmelt runoff volume in year 2.

217 In most cases, stormwater runoff volume correlates well linearly with precipitation and can
218 be estimated by precipitation depth. However, this relationship in the Tahoe Basin can be
219 influenced by other factors, such as precipitation type (e.g., rain, snow), interevent dry period
220 length, precipitation duration, presence/absence of man-made hillsides (also called cut slopes) or
221 naturally produced hillsides (also called native slopes), and slope and area of hillsides. For
222 example, stormwater runoff volumes can be significantly greater than estimated volumes at a site
223 with hillsides angling toward the road on one or both sides than at a site with no hillsides or
224 hillsides angling away from the road. Hillsides are pervious, so stormwater runoff from hillsides
225 does not start until surface soil on hillsides are saturated by rain. But, when surface soil on
226 hillsides are saturated with rain, stormwater starts to run off the surface and mix with runoff from
227 the road surface. Stormwater runoff from hillsides can also significantly increase FSP load.⁷

228 Stormwater volumes calculated from precipitation depth may overestimate the contribution
229 from hillsides for events with longer precipitation durations and longer interevent dry periods.
230 When interevent dry periods are longer, surface soils are dryer and it takes longer for runoff to
231 occur. To minimize uncertainties from these factors, the following equation was developed to
232 estimate stormwater runoff volume (V) from precipitation.

233

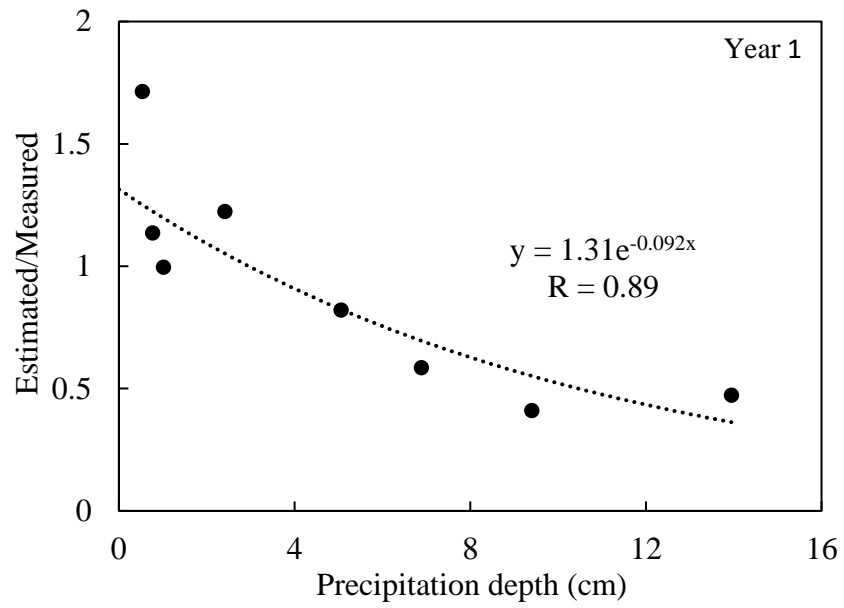
234
$$V = DA \times RF \times P \times C \times e^{-(k1 \times RD)} \times e^{-(k2 \times ID)} \quad (\text{Eq. 2})$$

235

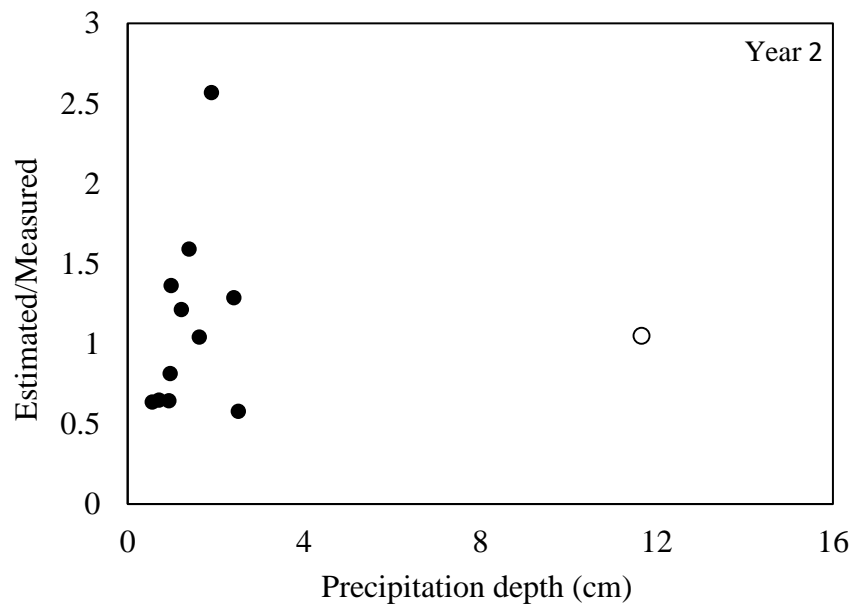
236 where V is estimated volume (m^3) of stormwater runoff, DA is drainage area (m^2), RF is fraction
237 of runoff that drains toward the side where the sampler was installed, P is precipitation depth (m)
238 for an event, C is runoff coefficient, RD (runoff duration) is time (hour) from start to end of
239 runoff, $k1$ is a constant of runoff duration, ID (interevent duration) is the dry period (days)
240 between the previous and current precipitation events, and $k2$ is a constant of interevent duration.
241 This equation was developed using data collected for the present study. Stormwater runoff
242 drainage area (DA) was calculated by multiplying length and width (pavement plus shoulders) of
243 the roads (Elks Club Drive and side streets) contributing runoff to the sampling stations. Runoff
244 fraction (RF) was determined by identifying the crown of the road and calculating the fraction of
245 surface runoff that would flow into drainage ditches that are connected to the sampling station.

246 Equation 2 does not incorporate the contribution from the adjacent hillside because it is
247 difficult to estimate stormwater runoff volumes from hillsides that is highly influenced by slope,
248 area, and surface condition of hillsides. Theoretical stormwater runoff volumes estimated using
249 equation 2 were compared to runoff volumes measured at the sampling site to determine the
250 influence of the adjacent hillside. If estimated volume is 2-fold lower than measured volume, it
251 can be inferred that runoff from the adjacent hillside accounts for 50% of the measured runoff
252 volume. When estimated volume to measured volume ratios are compared with precipitation
253 depth, a strong negative correlation is observed in year 1 (Figure 1). This indicates that the
254 contribution of stormwater runoff from the hillsides increased with increasing of precipitation.
255 When precipitation was less than 2.5 cm, estimated to measured volume ratios were greater than
256 1 in year 1, indicating that the adjacent hillsides was not likely saturated by rain and unlikely

257



258



259

260 **Figure 1.** Comparison of estimated to measured stormwater runoff volume ratios and precipitation
261 for stormwater runoff collected before (year 1) and after (year 2) pavement condition improvement.
262 Open circle in year 2 indicates an outlier.

263 contributed to stormwater runoff measured at the site. But stormwater runoff from the adjacent
264 hillsides accounted for about 50% of total volume when precipitation was greater than 8 cm. This
265 pattern was not observed in year 2 because precipitation was less than 2.5 cm for all events
266 except one.

267

268 **FSP concentrations and loads.** The significantly lower FSP concentrations observed in
269 year 2 clearly show the benefit of pavement condition improvement in reducing FSP load in
270 stormwater runoff. This indicates that pavement condition is an important factor to be included
271 in managing FSP load in stormwater runoff especially in the Lake Tahoe Basin. FSP
272 concentrations in stormwater runoff samples ranged from 19.1 mg/L to 297 mg/L in year 1 and
273 1.54 mg/L to 21.0 mg/L in year 2 (Table 1). These are within the range of FSP concentrations
274 observed at other sites in the Tahoe Basin.¹¹ Arithmetic mean FSP concentration was 47.4 ± 25.9
275 mg/L in year 1 and declined to 6.34 ± 3.60 mg/L in year 2. If values were outside of upper or
276 lower boundaries, they were regarded as outliers and not included in the calculation of arithmetic
277 mean concentrations. The upper and lower boundaries were calculated by adding 1.5 times of
278 interquartile range (IQR) to 75th percentile and subtracting 1.5 times of IQR from 25 percentile,
279 respectively. IQR is the difference between 75th and 25th percentiles. The ANOVA test shows
280 this reduction is statistically very significant ($p < 0.01$).

281 Volume weighted mean FSP concentration was 53.1 mg/L in year 1 and declined by 84% to
282 8.57 mg/L in year 2. The volume weighted mean FSP concentrations are 12% and 35% higher
283 than the arithmetic mean concentrations in years 1 and 2, respectively. Arithmetic mean FSP
284 concentration, which is an unweighted mean, may represent the overall FSP concentration less
285 accurately because the FSP concentration for each event is weighted equally regardless of

286 stormwater runoff volume. FSP concentrations in large and small events need to be weighted
287 more and less, respectively, to calculate the overall FSP concentrations accurately.

288 FSP load delivered by stormwater runoff was calculated by multiplying FSP concentration
289 and stormwater runoff volume of each event. FSP load ranged from 1.36 kg to 105 kg in year 1
290 and 0.05 kg to 1.08 kg in year 2 (Figure 2). Annual FSP loads calculated by multiplying the
291 volume weighted mean FSP concentrations by annual total stormwater runoff volumes ($5.72 \times$
292 10^6 L for year 1 and 3.15×10^6 L for year 2) were 303 kg in year 1 and 27 kg in year 2. For this
293 study, however, stormwater runoff samples were collected for 7 and 12 events in years 1 and 2,
294 respectively, that account for 70% and 50% (by volume) of all stormwater runoff in years 1 and
295 2, respectively. This means that FSP concentrations were not measured in 30% (year 1) and 50%
296 (year 2) of stormwater runoff and 100% of snowmelt runoff. Therefore, some uncertainties may
297 arise if the FSP concentrations measured from the collected stormwater samples are applied to
298 the rest of the runoff.

299 As an alternative, FSP concentrations can be estimated using turbidity of stormwater runoff
300 measured on site using digital sensors. Heyvaert et al.¹¹ compiled the results of the monitoring
301 conducted in the Tahoe Basin between 1992 and 2012 and found that turbidity of stormwater
302 runoff had a strong positive correlation with FSP concentrations expressed in mass (mg/L) and
303 developed the following equation

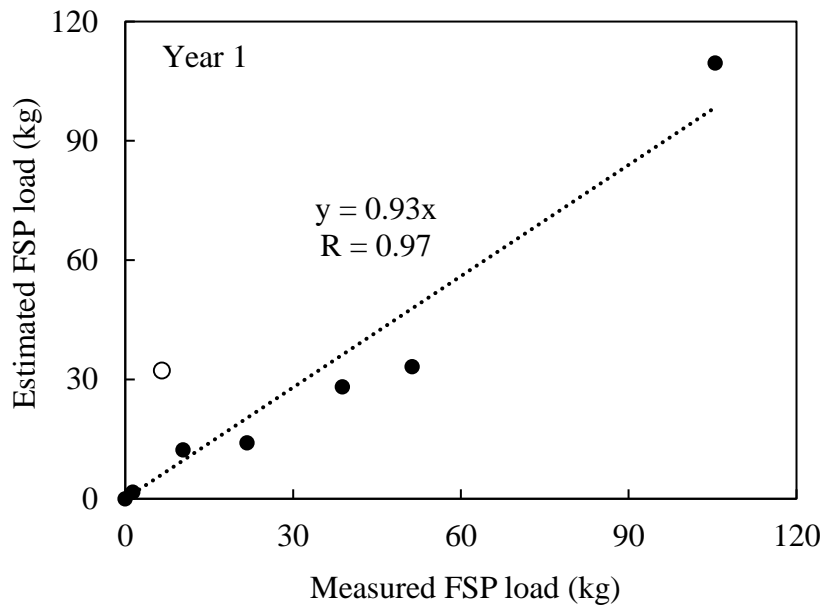
304

$$305 \text{ FSP concentration (mg/L)} = 10^{(-k + 1.08 \cdot \text{Log T})} \quad (\text{Eq. 3})$$

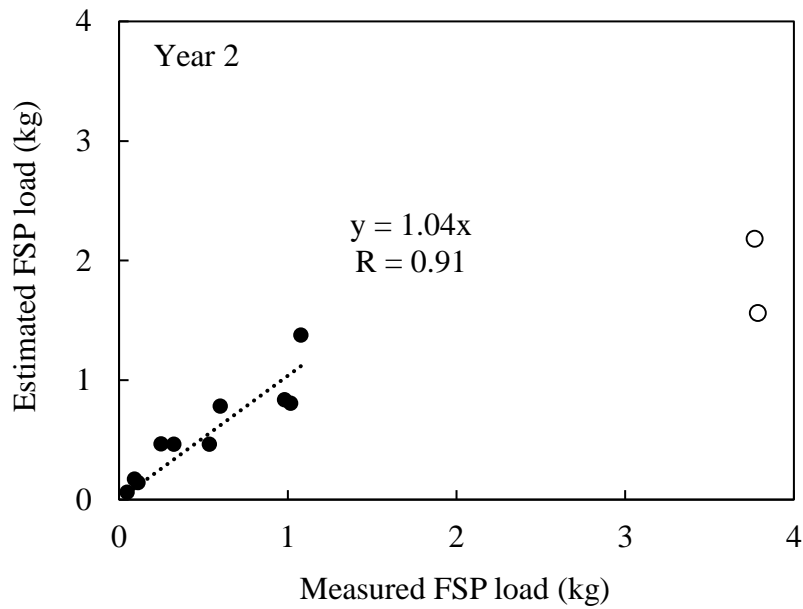
306

307 where k is a conversion constant and T is real-time turbidity (NTU) measured on site.

308



309



310

311 **Figure 2.** Comparison of measured and estimated FSP loads in stormwater runoff collected before
 312 (year 1) and after (year 2) pavement condition improvement. Outliers (open circles) were not
 313 included in the regression analysis.

314

315 The FSP loads estimated using the real-time turbidity measured every 5 minutes on site were
316 compared to the gravimetrically measured FSP loads in runoff samples (Figure 2). They showed
317 a very strong positive correlation for both years. This indicates that the annual FSP load
318 estimated from continuous turbidity measured in-situ is reliable. For both years, outliers were not
319 included in determining correlation coefficients. In a couple of events, large differences between
320 the measured and the estimated FSP loads were observed (Figure 2). The most likely explanation
321 is unexpected malfunctions of the turbidity sensor and the water flow sensor, which is often seen
322 in continuous field sampling.

323 The continuous real-time turbidity measured on site was converted to FSP concentrations in
324 stormwater and snowmelt runoff and then multiplied by real-time runoff volume to calculate FSP
325 load, which was added up for the whole year to calculate the annual (October 1-September 30)
326 cumulative FSP loads for years 1 and 2. The estimated annual cumulative FSP load delivered
327 was 293 kg in year 1 and declined by 87% to 36.7 kg in year 2. Annual cumulative runoff
328 volume in year 2 was only 5% less than year 1, indicating that the reduction in annual FSP load
329 was associated with the reduction in FSP concentration in stormwater runoff.

330

331 **Sources of fine sediment particles.** The major sources of FSP in stormwater runoff were
332 pavement materials (aggregates and asphalt binder), native soil, traction abrasives, and
333 vegetation debris. These four major sources, combined, accounted for $96.1 \pm 1.4\%$ of the total
334 FSP load in year 1 and $91.7 \pm 1.8\%$ in year 2 (Table 2). Pavement condition improvement
335 contributed to significant reduction in FSP load from all these major sources. FSP load from
336 these four sources, combined, declined from 291 kg in year 1 to 24.8 kg in year 2.

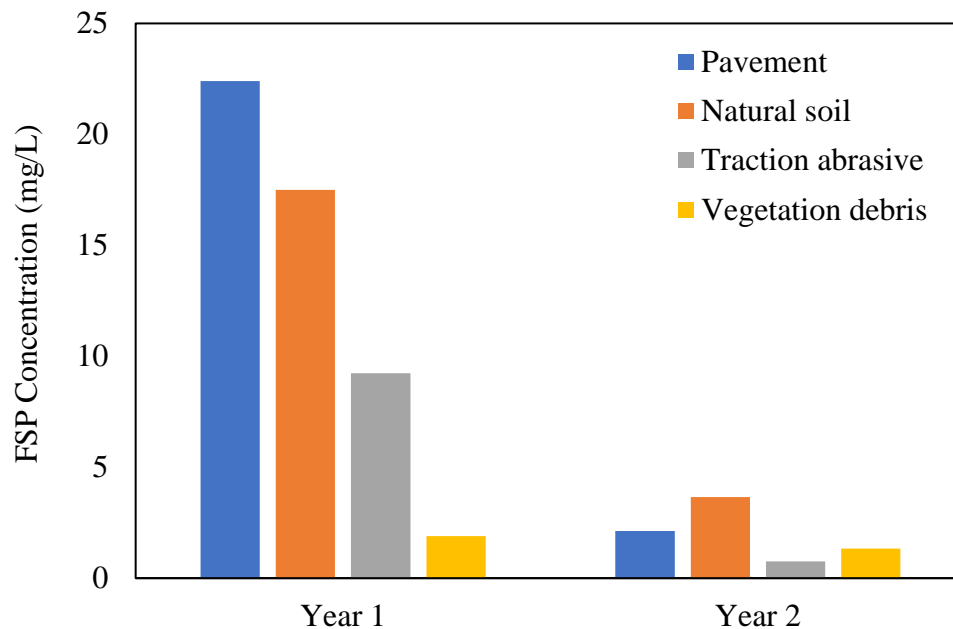
337

338 **Table 2.** Sources of FSP in stormwater runoff collected before (year 1) and after (year 2) pavement
 339 condition improvement.

	Year 1		Year 2	
	Contribution (%)	VWM* (mg/L)	Contribution (%)	VWM (mg/L)
Natural Soil	33.0 ± 6.8	17.5	42.6 ± 6.7	3.65
Pavement (aggregate + binder)	42.2 ± 9.4	22.4	24.8 ± 5.9	2.12
Traction abrasive	17.4 ± 5.4	9.23	8.9 ± 3.7	0.76
Vegetation debris	3.6 ± 2.4	1.89	15.5 ± 5.5	1.33
Atmospheric deposition	3.0 ± 1.4	1.59	4.9 ± 1.7	0.42
Tire	0.7 ± 0.2	0.37	3.2 ± 2.6	0.27
Engine Oil	0.2 ± 0.0	0.11	0.2 ± 0.0	0.02
Brake Pad and Drum	0.03 ± 0.02	0.02	0.12 ± 0.2	0.01
Lead tire balancing weight	< 0.0001	< 0.00001	< 0.0001	< 0.00001

*VWM: Volume weighted mean concentration

340
 341 Before pavement rehabilitation, wear of asphalt pavement materials was the primary source
 342 of FSP in stormwater runoff. Asphalt pavement materials accounted for 42.2 ± 9.4% of the FSP
 343 load in year 1 and declined to 24.8 ± 5.9% in year 2. Changes in contribution percentages do not
 344 reflect actual changes in FSP loads from each source because the percentages are relative values.
 345 When converted to volume weighted mean concentration, pavement rehabilitation reduced FSP
 346 from pavement wear by 91%, from 22.4 mg/L in year 1 to 2.12 mg/L after pavement
 347 rehabilitation (Figure 3). Asphalt pavement materials consist of aggregates, which include
 348 crushed rocks, natural gravels, and sand-soil mixtures, and an asphalt binder, also known as
 349 bitumen, which is a general description for the adhesive or glue that is used to bind the
 350 aggregates together in pavements.^{12, 13}



352

353 **Figure 3.** Volume weighted mean concentrations of FSP from major sources before (year 1) and
 354 after (year 2) pavement condition improvement.

355

356 Asphalt pavements constitute the surface layer of the majority of the roads in the Lake Tahoe
 357 Basin. The primary mechanism of FSP generation from the pavement surface is friction between
 358 pavement materials and vehicle tires with and without snow chains and steel blades mounted on
 359 snow removal equipment such as snow plows and snow blowers. Aging and damage from
 360 repeated loading and environmental stresses over time accelerate the release of FSP. As asphalt
 361 binder slowly ages, it becomes progressively stiffer and more brittle, and the pavement surface
 362 starts losing aggregates and the pavement becomes less durable.¹² Temperature also has an effect
 363 on asphalt binder. At low temperatures (e.g., below freezing) commonly observed in winter in
 364 the Tahoe Basin, asphalt binder becomes very stiff and less resistant to stresses.¹³⁻¹⁵ These

365 changes in the binder characteristics make the pavement surface experience a faster loss of
366 binder and aggregates through weathering and cracking (Figure S9). Snow removal practices
367 also damage the pavement surface substantially (Figures S3 and S4) and accelerate the
368 generation of FSP from pavement materials. So, a greater amount of FSP is likely to be
369 generated from older and more damaged pavements commonly observed in the Tahoe Basin. In
370 El Dorado County, asphalt pavements in poor or fail condition with a PCI of 50 or lower account
371 for more than 50% of all roads (Figure S10), indicating that improvement of pavement in poor or
372 fail condition can significantly reduce FSP loads from pavements.

373 Percent contribution of traction abrasives was significantly reduced from $17.4 \pm 5.4\%$ in year
374 1 to $8.9 \pm 3.7\%$ in year 2. Volume weighted mean concentration of FSP from traction abrasives
375 declined by 92% from 9.23 mg/L in year 1 to 0.76 mg/L in year 2. This reduction in FSP
376 concentration cannot be explained by the amount of traction abrasives applied in years 1 and 2.
377 The total annual amount of traction abrasives applied on the roads in the County of El Dorado
378 were significantly greater in year 2 (450 tons) than in year 1 (318 tons), probably due to more
379 precipitation between December and March in year 2 when the ambient temperatures were often
380 below freezing. Therefore, this reduction in FSP originating from traction abrasives was likely
381 associated with pavement condition improvement. Pavement in poor condition with many cracks
382 and potholes, like Elks Club Drive in year 1, can retain greater amounts of FSP associated with
383 traction abrasives. Additionally, road sweeping is less effective in removal of FSP on pavement
384 in poor condition,^{16, 17} so a significant fraction of FSP originating from traction abrasives was
385 likely retained on the pavement and washed off by stormwater runoff in year 1.

386 Percent contribution of native soil increased from $33.0 \pm 6.8\%$ in year 1 to $42.6 \pm 6.7\%$ in
387 year 2 after pavement habilitation. Again, this is just a proportional increase and does not mean

388 that the FSP loads originating from native soil increased after pavement rehabilitation, as these
389 are relative percentages. Volume weighted mean concentration of FSP from native soil declined
390 by 79% from 17.5 mg/L to 3.65 mg/L. FSP associated with native soil originates from subgrade
391 and narrow and partially vegetated hillsides with a gentle slope only on the north side of Elks
392 Club Drive. Many roads in the Tahoe Basin have hillsides on one or both sides of roads because
393 roads are constructed through hilly terrain. Road construction in hilly areas removes stabilized
394 topsoil and exposes nutrient-poor subsoil, so cut slopes (man-made hillsides) are typically a bare
395 or partially vegetated surface.¹⁸ Erosion from bare cut slopes was nearly an order of magnitude
396 greater than erosion from native slopes in the Lake Tahoe Basin.^{19,20} A four-year cumulative
397 erosion study in forest cut slopes showed that bare slopes produced 5.5 times more sediment than
398 slopes with native species vegetation.²¹ Repeated freeze-thaw cycle is also one of the main
399 disintegrating forces for soil aggregates, resulting in increased soil erosion.^{22,23}

400 A significant portion of the FSP was also likely originated from subgrade, a layer of
401 compacted roadbed soil underneath of pavement, which can be disturbed by vehicles and winter
402 road maintenance practices (e.g., snow removal). As subgrade is saturated by water and
403 experiences freeze-thaw cycles repeatedly, subgrade loses compaction and becomes less
404 consolidated. FSP contained in subgrade can then be quickly pumped to the pavement surface
405 through cracks and potholes. This study, however, did not quantify the proportion of FSP in
406 roadway stormwater runoff that originated from subgrade because it is difficult to differentiate
407 hillside soil and subgrade using element composition.

408 Percent contribution of plant debris (e.g., leaves, cones, needles, twigs, stems and foliage of
409 non-woody plants) increased from $3.6 \pm 2.4\%$ in year 1 to $15.5 \pm 5.5\%$ in year 2 after pavement
410 habilitation. This also does not mean the FSP loads originating from plant debris increased after

411 pavement rehabilitation. Volume weighted mean concentration of FSP from plant debris declined
412 by 30% from 1.89 mg/L to 1.33 mg/L. This is the lowest reduction among the four major
413 sources.

414 FSP can also be produced from plant debris that has fallen on the pavement surface or
415 hillside. Plant debris on the pavement surface can be pulverized by tire abrasion. If pulverization
416 by tires was the primary source of FSP originating from plant debris, the reduction percentage of
417 FSP from vegetation debris should be similar to the reduction observed in traction abrasives that
418 declined by 92%. The reduction (30%) observed in plant debris means that a much greater
419 portion of FSP originating from plant debris was introduced from the hillside. Plant debris from
420 the hillside can be transformed into FSP through microbial decomposition, mechanical
421 breakdown, and chemical actions. Pavement condition does not influence washoff of FSP
422 originating from plant debris from the hillside.

423

424 **First Flush Phenomenon.** It is common to observe the first flush phenomenon for pollutants
425 in stormwater runoff from urban roadways in excellent/good condition.²⁴⁻²⁶ Two different types
426 of first flush phenomenon have been used to describe transport of pollutants by stormwater
427 runoff. Concentration-based first flush can be defined as a disproportionately higher
428 concentrations of pollutants in the early phase compared to the remaining phases of a rain event.
429 Another type of first flush is mass-based first flush that can be defined as disproportionately
430 higher load of pollutants in the early phase. Most groups dealing with FSP in stormwater runoff
431 in the Lake Tahoe Basin prefer to use load rather than concentration. So, this study uses the term
432 load-based first flush (LFF).

433 LFF can be presented by numerical ratios and/or graphs.^{25, 26} The unitless LFF ratios can be
434 calculated by dividing the cumulative fraction of FSP load by the cumulative fraction of runoff
435 volume measured at the same time point. Different numerical cutoffs have been used to
436 determine the presence of the first flush phenomenon. Some studies defined the first flush as an
437 80% or greater fraction of pollutants transported during the first 20% or 30% of runoff volume,
438 which can be described as an 80/20 or 80/30 first flush.^{24, 25} Other studies described the first
439 flush as 50/25 or 40/20.²⁷ LFF ratios of 80/20, 80/30, and 50/25 are 4.0, 2.7, and 2.0,
440 respectively. For this study, 40/20 or an LFF ratio of 2.0, was used as a cutoff to minimize
441 influence of FSP from hillside on the presence of the first flush phenomenon. Because many
442 roads in the Lake Tahoe Basin have hillsides or cut slopes on one or both sides, FSP from natural
443 surface soil from hillsides or cut slopes can contribute significantly to the FSP load in
444 stormwater runoff. Asphalt pavement is impervious, so stormwater runoff is created shortly after
445 rain starts. However, hillsides are pervious, so stormwater runoff does not start until surface soils
446 on hillsides are saturated by rain, and the contribution of FSP from hillsides is likely delayed
447 compared to the contribution from pavement.

448 LFF ratios at 20% of runoff volume (LFF₂₀ ratios) ranged from 1.07 to 3.97 in year 1 and
449 0.73 to 2.82 in year 2. The first flush phenomenon was observed more frequently in year 1.
450 Different precipitation patterns in rain events are likely responsible for this wide range of the
451 LFF ratios. The input of FSP from the hillsides can also contribute to the wide range of LFF₂₀
452 ratios. Significantly higher LFF₂₀ ratios were observed in year 1 (1.96 ± 1.13) than in year 2
453 (1.15 ± 0.65) probably because FSP loads from pavement were much higher and the contribution
454 of FSP from hillside soils in the later phase of the rain events was relatively lower in year 1.

455 The first flush phenomenon can also be presented visually in graphs. The presence of the first
456 flush can be illustrated when a data line representing the dimensionless cumulative FSP load
457 against the dimensionless cumulative of runoff volume is significantly above a theoretical line
458 representing a synchronistic cumulative increase in FSP loads at the same rate as runoff volumes
459 (Figure S11). A data line close to the theoretical line indicates no presence of the first flush.

460

461 **Lake Clarity Credit.** In the Tahoe Basin, FSP reduction in roadway stormwater runoff is
462 converted to Lake Clarity Credit under the TMDL Program's 65-year plan to restore Lake
463 Tahoe's clarity to 33 m.³ A 100 kg load reduction in FSP is equal to 1.1 credit.³ Each municipal
464 jurisdiction in the Tahoe Basin is required to earn a specific number of credits each year to meet
465 the lake clarity goal established by TMDL. The results of this study facilitate an estimation of
466 how many credits can be earned when pavements in poor condition are improved. The results of
467 this study indicate that the reduction (256 kg) in annual FSP load from the study site (0.52 km of
468 pavement) is equal to 2.8 credits or 5.4 credits per 1 km of pavement. A pavement surface slope
469 survey indicated that 70% of stormwater runoff ran toward the side where the sampling station
470 was installed. So, when combined with the FSP reduction associated with the remaining 30% of
471 runoff that ran to the other side of the road, this pavement rehabilitation is estimated to provide
472 7.7 credits per 1 km of pavement in the first year after the pavement rehabilitation. The reduction
473 in FSP load from the new asphalt overlay (1.3 km) installed for this pavement rehabilitation
474 project is equivalent to 10 credits. Further evaluations are required to determine whether earning
475 credit from pavement condition improvement can be blended into the Road Rapid Assessment
476 Method (RoadRAM), a field observation and data management tool that has been implemented
477 in the Tahoe Basin to rapidly assess relative pavement condition of large areas of roads.²⁸ As the

478 new asphalt pavement ages, FSP loads are expected to gradually increase. But FSP loads from
479 old asphalt pavement are likely to increase at a faster rate as pavement ages. Therefore, the same
480 credit may be used for estimating FSP load reduction for many years following the installation of
481 the new asphalt overlay.

482

483 **CONCLUSIONS**

484 This study provides clear evidence that pavement condition improvement is highly beneficial
485 in reducing FSP in roadway stormwater runoff, suggesting that pavement condition and FSP load
486 in stormwater runoff need to be included in cost-benefit analyses for pavement asset
487 management. FSP load reduction associated with pavement condition improvement may also
488 help jurisdictions earn Lake Clarity Credits. Until now, the impacts of pavement condition on
489 FSP load in stormwater runoff has not received enough attention and there has been a lack of
490 information robust enough to be used for more accurate cost-benefit analyses. Additional studies
491 are required to determine what pavement condition index should trigger replacement of damaged
492 roads. Effectiveness of sweeping in removing FSP from pavements with different condition
493 indices also needs to be measured to estimate the maximum benefits of pavement condition
494 improvement. Impacts of other factors such as strength of pavement materials (binder and
495 aggregates) and road sweeping frequency on the reduction of FSP loads also need to be studied.

496

497 **ACKNOWLEDGEMENTS**

498 We would like to give special thanks Cara Moore and Raph Townsend at Tahoe Resource
499 Conservation District, Brendan Ferry, Michael Broadhurst, Matt Moody, and Dan Kikkert at El

500 Dorado County, and Janyl Madykova at Texas Southern University for their critical support for
501 sampling station construction, stormwater runoff collection, laboratory sample pretreatment,
502 artificial runoff simulation, and other technical assistance and suggestions. This project could not
503 have been completed without their valuable help. This project was partially supported by NSF
504 Research Infrastructure for Science and Engineering grant (HRD 1829181).

505

506 **REFERENCES**

- 507 1. Swift, T. J., Perez-Losada, J., Schladow, S. G., Reuter, J. E., Jassby, A. D., & Goldman, C.
508 R. (2006). Water clarity modeling in Lake Tahoe: Linking suspended matter characteristics
509 to Secchi depth. *Aquatic Sciences*, 68, 1-15.
- 510 2. Sahoo, G. B., Nover, D. M., Reuter, J. E., Heyvaert, A. C., Riverson, J., & Schladow, S. G.
511 (2013). Nutrient and particle load estimates to Lake Tahoe (CA–NV, USA) for Total
512 Maximum Daily Load establishment. *Science of the total environment*, 444, 579-590.
- 513 3. Lahontan Water Quality Control Board (LWQCB) & Nevada Division of Environmental
514 Protection (NDEP). 2011. *Lake Clarity Crediting Program Handbook: for Lake Tahoe*
515 *TMDL Implementation v1.0*. Prepared by Environmental Incentives, LLC. South Lake Tahoe,
516 CA, USA.
- 517 4. Kupiainen, K. (2007). Road dust from pavement wear and traction sanding. Finnish
518 Environment Institute, Helsinki, Finland.
- 519 5. Qualls, R. G., & Heyvaert, A. C. (2017). Accretion of nutrients and sediment by a
520 constructed stormwater treatment wetland in the Lake Tahoe Basin. *JAWRA Journal of the*
521 *American Water Resources Association*, 53, 1495-1512.
- 522 6. Wigart, R., & Ferry, B. (2015). Analysis of Particle Size and Particle Distribution of
523 Volcanic Cinders and Decomposed Granite for TMDL Load Reduction Crediting.
524 Department of Transportation, El Dorado County, CA, USA.
- 525 7. Hwang, H-M., Fiala, M., Wigart, R., Townsend, R., & Edirveerasingam, V. (2017). Sources
526 of fine sediment particles (< 20 µm) in roadway runoff in the Lake Tahoe Basin. Final report.
527 Prepared for the USDA Forest Service, Pacific Southwest Research Station, Albany, CA,
528 USA.

- 529 8. EIP, (2021). 2020 Accomplishments. Lake Tahoe Environmental Improvement Program,
530 South Lake Tahoe, CA, USA.
- 531 9. ASTM D6433-20. Standard practice for roads and parking lots pavement condition index
532 surveys. ASTM International, West Conshohocken, PA, USA.
- 533 10. Mackey, E. A., Christopher, S. J., Lindstrom, R. M., Long, S. E., Marlow, A. F., Murphy, K.
534 E., ... & Nebelsick, J. (2010). Certification of three NIST renewal soil standard reference
535 materials for element content: SRM 2709a San Joaquin Soil, SRM 2710a Montana Soil I, and
536 SRM 2711a Montana Soil II. *NIST Special Publication*, 260, 1-39.
- 537 11. Heyvaert, A. C., 2NDNATURE, & Reuter, J. E. (2015). Analysis of turbidity as a surrogate
538 indicator for fine sediment particle concentrations in the Tahoe Basin. Final report. Prepared
539 for the USDA Forest Service, Pacific Southwest Research Station, Albany, CA, USA.
- 540 12. Lavin, P. (2003). Asphalt Pavements: A Practical Guide to Design, Production and
541 Maintenance for Engineers and Architects. Taylor & Francis, Oxford, UK.
- 542 13. Speight, J. G. (2015). Asphalt Materials Science and Technology. Butterworth-Heinemann,
543 Oxford, UK.
- 544 14. Lamothe, S., Perraton, D., & Benedetto, H. D. (2017). Degradation of hot mix asphalt
545 samples subjected to freeze-thaw cycles and partially saturated with water or brine. *Road*
546 *Materials and Pavement Design*, 18, 849-864.
- 547 15. Ahmad, T., & Khawaja, H. (2018). Review of low-temperature crack (LTC) developments in
548 asphalt pavements. *International Journal of Multiphysics*, 12, 169-187.
- 549 16. Pitt, R. E., Williamson, D., Voorhees, J., & Clark, S. (2005). Review of historical street dust
550 and dirt accumulation and washoff data. *Journal of Water Management Modeling*, 223, 203-
551 246.

- 552 17. Amato, F., Querol, X., Johansson, C., Nagl, C., & Alastuey, A. (2010). A review on the
553 effectiveness of street sweeping, washing and dust suppressants as urban PM control
554 methods. *Science of the total environment*, 408, 3070-3084.
- 555 18. Navarro-Hevia, J., Lima-Farias, T. R., de Araújo, J. C., Osorio-Peláez, C., & Pando, V.
556 (2016). Soil erosion in steep road cut slopes in Palencia (Spain). *Land Degradation &*
557 *Development*, 27, 190-199.
- 558 19. Grismer, M. E., & Hogan, M. P. (2005). Simulated rainfall evaluation of revegetation/mulch
559 erosion control in the Lake Tahoe basin: 2. Bare soil assessment. *Land Degradation &*
560 *Development*, 16, 397-404.
- 561 20. Grismer, M.E., Ellis, A.L. and Fristensky, A. (2008). Runoff sediment particle sizes
562 associated with soil erosion in the Lake Tahoe Basin, USA. *Land Degradation &*
563 *Development*, 19, 331-350.
- 564 21. Grace III, J. M. (2002). Effectiveness of vegetation in erosion control from forest road
565 sideslopes. *Transactions of the American Society of Agricultural Engineers*, 45, 681.
- 566 22. Edwards, L. M. (2013). The effects of soil freeze–thaw on soil aggregate breakdown and
567 concomitant sediment flow in Prince Edward Island: A review. *Canadian Journal of Soil*
568 *Science*, 93, 459-472.
- 569 23. Wang, Q., Qi, J., Qiu, H., Li, J., Cole, J., Waldhoff, S., & Zhang, X. (2021). Pronounced
570 increases in future soil erosion and sediment deposition as influenced by Freeze–Thaw
571 Cycles in the Upper Mississippi River Basin. *Environmental Science & Technology*, 55,
572 9905-9915.

- 573 24. Bertrand-Krajewski, J. L., Chebbo, G., & Saget, A. (1998). Distribution of pollutant mass vs
574 volume in stormwater discharges and the first flush phenomenon. *Water research*, 32, 2341-
575 2356.
- 576 25. Sansalone, J. J., & Cristina, C. M. (2004). First flush concepts for suspended and dissolved
577 solids in small impervious watersheds. *Journal of environmental engineering*, 130, 1301-
578 1314.
- 579 26. Stenstrom, M. K., & Kayhanian, M. (2005). First flush phenomenon characterization (No.
580 CTSW-RT-05-073.02. 6). California Department of Transportation, Sacramento, CA, USA.
- 581 27. Deletic, A. (1998). The first flush load of urban surface runoff. *Water research*, 32, 2462-
582 2470.
- 583 28. 2NDNATURE, NHC, and Environmental Incentives. (2015). Road rapid assessment
584 methodology (Road RAM) user manual v2, Tahoe Basin. Prepared for the Nevada Division
585 of Environmental Protection, Carson City, NV, USA and Lahontan Regional Water Quality
586 Control Board, Victorville, CA, USA.

587

SUPPORTING INFORMATION

Impacts of Pavement Condition on Fine Sediment Particle Load in Roadway Stormwater Runoff

Hyun-Min Hwang^{1*}, Russell Wigart², Andrea Buxton³

¹Dept. of Environmental Science, Texas Southern University, Houston, Texas, USA

²Tahoe Planning and Stormwater Division, El Dorado County, Placerville, California, USA
(russell.wigart@edcgov.us)

³Tahoe Resource Conservation District, South Lake Tahoe, California, USA
(abuxton@tahoercd.org)

*Corresponding author

Description of Supporting Information

Figure S1. Historical changes in Lake Tahoe clarity. This image was retrieved from the website of Tahoe Environmental Research Center, University of California, Davis (www.terc.ucdavis.edu).

Figure S2. Annual usage of traction abrasives in El Dorado County since the winter of 2001. The dashed regression line represents a gradual decline of abrasive usage at a rate of 52 tons per year. Usage data was retrieved from Wigart and Ferry (2015).

Figure S3. Snow plow equipped with a metal blade (left) and rotary blades mounted on a snow blower (right), operated by El Dorado County to remove snow from roads.

Figure S4. Pavement damage caused by snow plows (left) and rotary blades (right). A mechanical pencil was placed to show the scale of the damage.

Figure S5. Aerial view of the study site and locations of sampling stations.

Figure S6. Pavement condition of Elks Club Drive before (left) and after (right) the installation of new asphalt overlay.

Figure S7. Sampling stations installed on Elks Club Drive for stormwater runoff collection before (year 1, left) and after (year 2, right) pavement rehabilitation.

Figure S8. Daily precipitation (rain and snow) and ambient atmospheric temperature recorded near the stormwater runoff collection site in year 1 (October 1, 2017-July 30, 2018) and year 2 (October 1, 2018-July 30, 2019).

Figure S9. Fatigue cracks (left) and severely enlarged cracks (right) developed on asphalt pavement surface on Elks Club Drive in County.

Figure S10. PCI of residential traffic roads in El Dorado County. Green, light green, orange, and red colors indicate roads in excellent/good (PCI: 70-100), at risk (PCI: 50-70), poor (PCI: 25-50), and failing (PCI: 0-25) conditions, respectively.

Figure S11. Comparison of the cumulative fractions of FSP load and runoff volume in stormwater runoff samples. Dashed line indicates theoretical synchronistic cumulative increases in FSP load at the same rate as runoff volume.

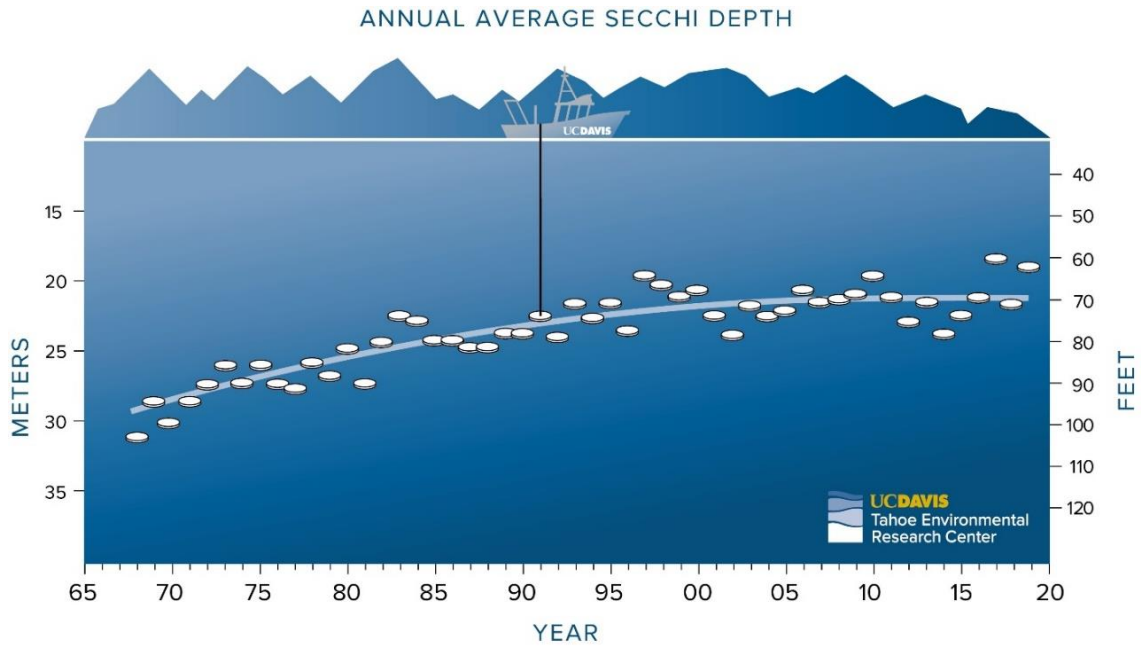


Figure S1. Historical changes in Lake Tahoe clarity. This image was retrieved from the website of Tahoe Environmental Research Center, University of California, Davis (www.terc.ucdavis.edu).

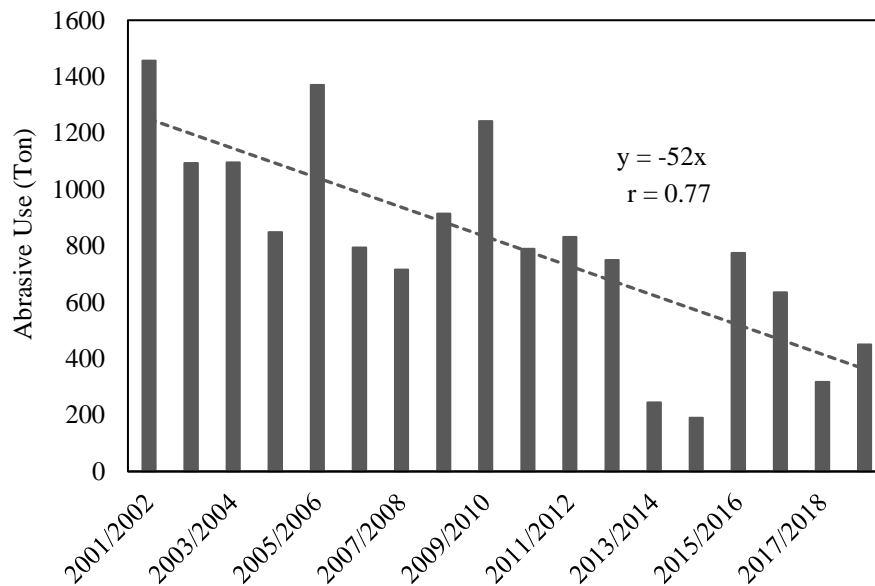


Figure S2. Annual usage of traction abrasives in El Dorado County since the winter of 2001. The dashed regression line represents a gradual decline of abrasive usage at a rate of 52 tons per year. Usage data was retrieved from Wigart and Ferry (2015).



Figure S3. Snow plow equipped with a metal blade (left) and rotary blades mounted on a snow blower (right), operated by El Dorado County to remove snow from roads.



Figure S4. Pavement damage caused by snow plows (left) and rotary blades (right). A mechanical pencil was placed to show the scale of the damage.



Figure S5. Aerial view of the study site and locations of sampling stations.



Figure S6. Pavement condition of Elks Club Drive before (left) and after (right) the installation of new asphalt overlay.



Figure S7. Sampling stations installed on Elks Club Drive for stormwater runoff collection before (year 1, left) and after (year 2, right) pavement rehabilitation.

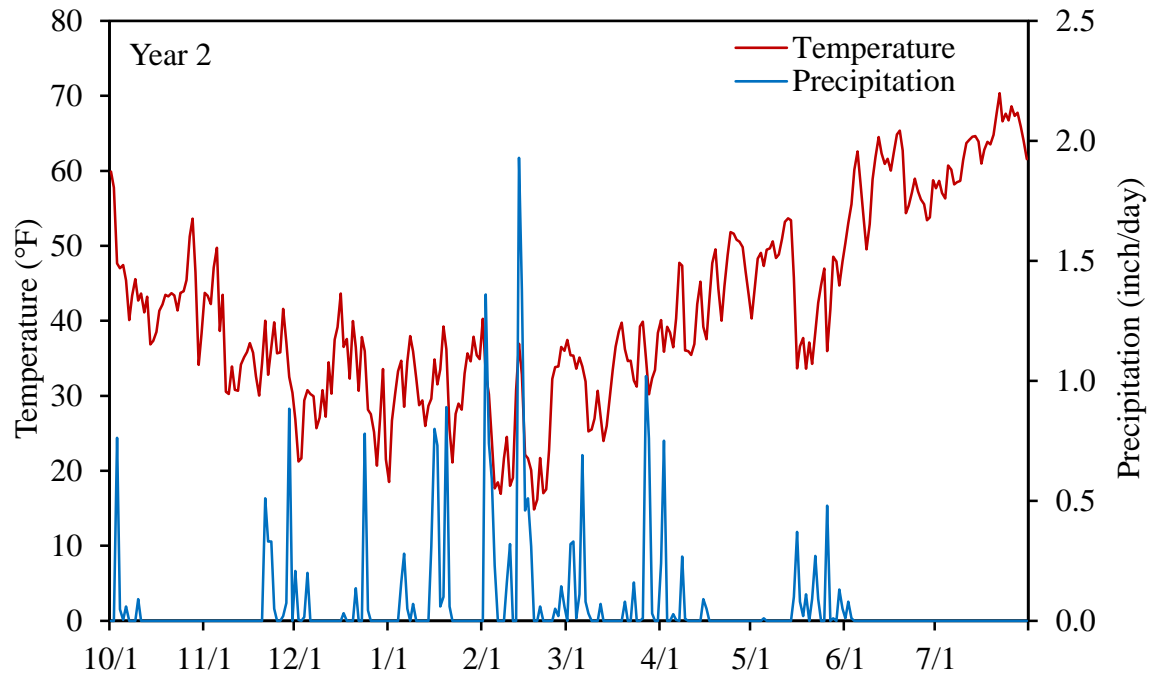
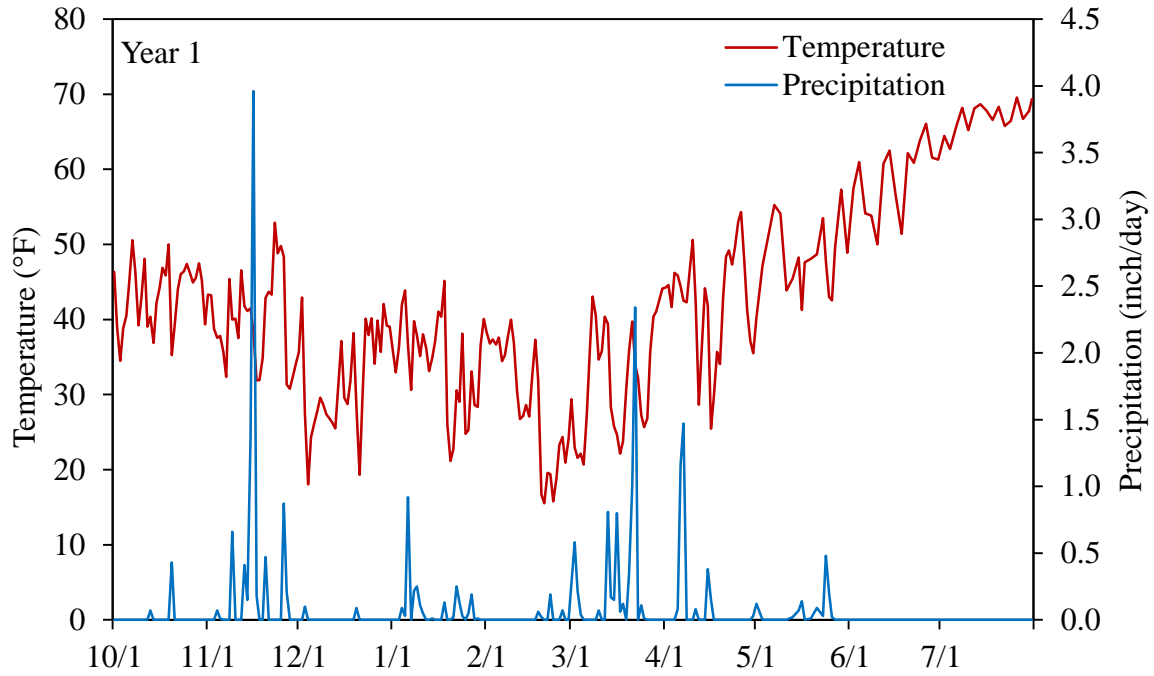


Figure S8. Daily precipitation (rain and snow) and ambient atmospheric temperature recorded near the stormwater runoff sampling site in year 1 (October 1, 2017-July 30, 2018) and year 2 (October 1, 2018-July 30, 2019).

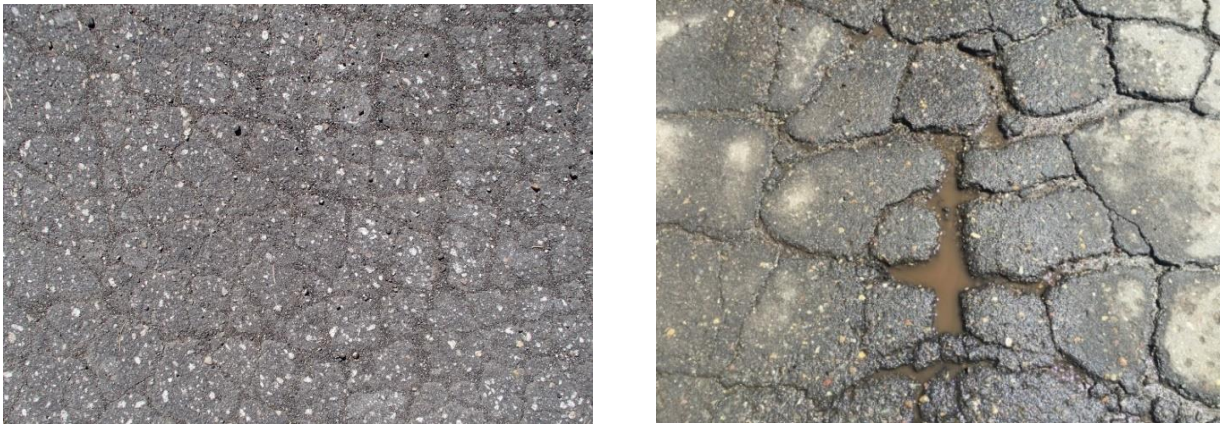


Figure S9. Fatigue cracks (left) and severely enlarged cracks (right) developed on asphalt pavement surface on Elks Club Drive in County.

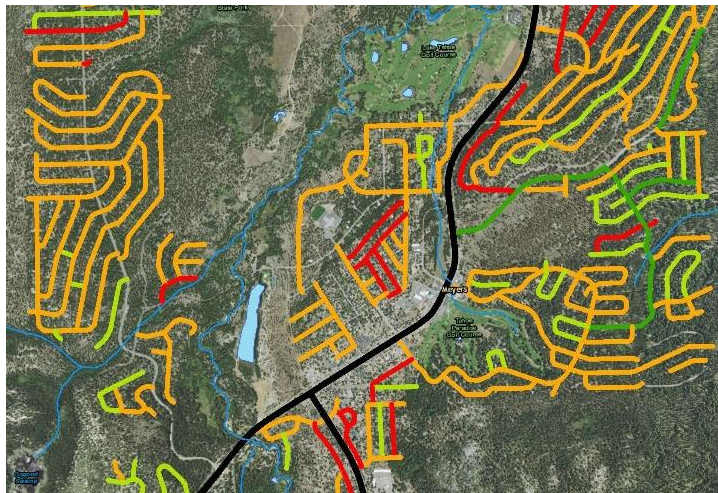


Figure S10. PCI of residential traffic roads in County. Green, light green, orange, and red colors indicate roads in excellent/good (PCI: 70-100), at risk (PCI: 50-70), poor (PCI: 25-50), and failing (PCI: 0-25) conditions, respectively. Photo credit: NCE.

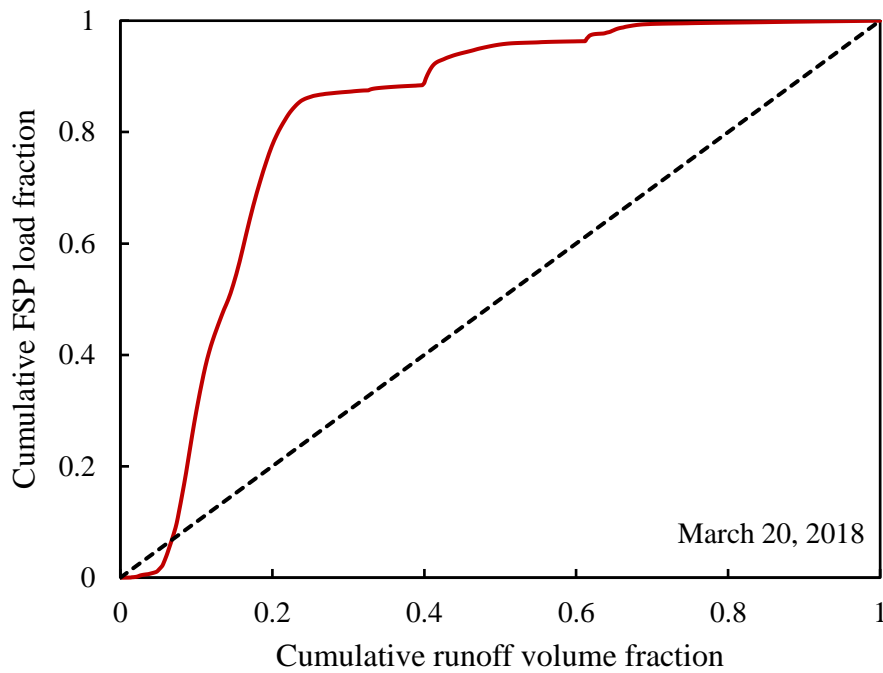
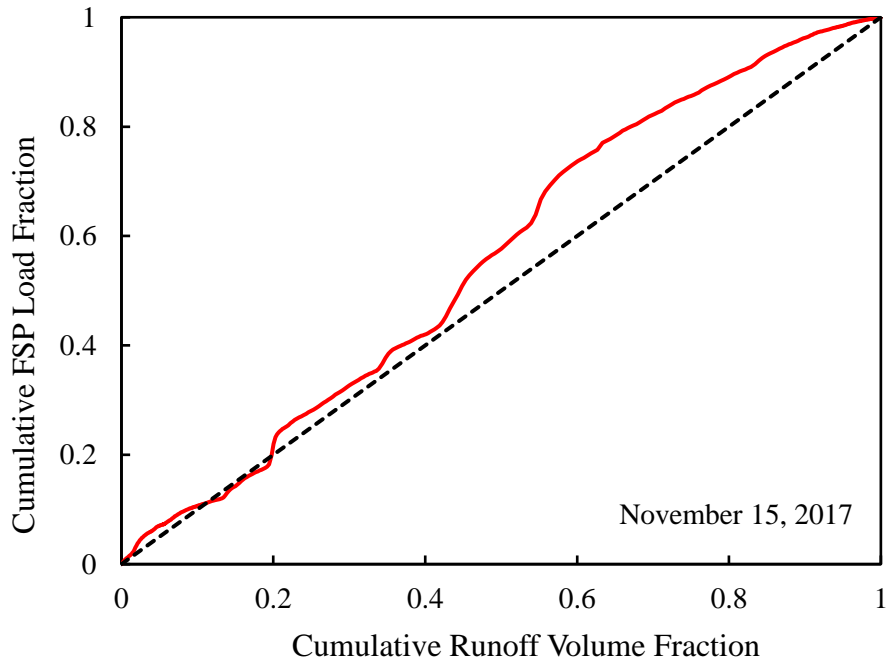


Figure S11. Comparison of the cumulative fractions of FSP load and runoff volume in stormwater runoff samples. Dashed line indicates theoretical synchronistic cumulative increases in FSP load at the same rate as runoff volume.